CMB Anisotropies from Collapsing Textures

Work in collaboration with J. Urrestilla

Kepa Sousa

Departamento de Física Teórica e Historia de la Ciencia
UPV/EHU.

kepa.sousa@ehu.es

University of Sussex, 27/01/2014

Outline

Introduction

- Textures are a class of topological defects.
- They are formed generically in cosmological models where a non-abelian global symmetry is spontaneously broken.
- Should the ΛCDM be augmented with textures?:
  - *Cruz et al. '08,'09* showed through bayesian analysis that a cosmic texture is consistent with the CMB anomaly know as the "Cold Spot".
  - Other possibilities: Sunyaev-Zeldovic effect or a large void.
  - Other works show discrepancies: *Feeney et al. '12*.

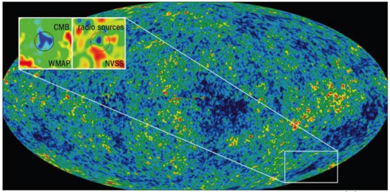

Introduction

- Textures are a class of topological defects.
- They are formed generically in cosmological models where a non-abelian global symmetry is spontaneously broken.
- Should the ΛCDM be augmented with textures?:
  - *Cruz et al. '08,'09* showed through bayesian analysis that a cosmic texture is consistent with the CMB anomaly know as the "Cold Spot".
  - Other possibilities: Sunyaev-Zeldovic effect or a large void.
  - Other works show discrepancies: *Feeney et al. '12*.

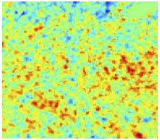

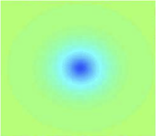

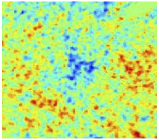

Introduction

- Textures are a class of topological defects.
- They are formed generically in cosmological models where a non-abelian global symmetry is spontaneously broken.
- Should the ΛCDM be augmented with textures?:
  - *Cruz et al. '08,'09* showed through bayesian analysis that a cosmic texture is consistent with the CMB anomaly know as the "Cold Spot".
  - Other possibilities: Sunyaev-Zeldovic effect or a large void.
  - Other works show discrepancies: *Feeney et al. '12*.

- All these analysis rely on the existing predictions on the anisotropy pattern produced by global textures.
- They use a very idealized analytical solution, (spherical symmetry and self similar collapse) *Turok et al. '90*
- which is known to be unrealistic *Borrill et al. '92*.

Topological Defects
Kibble mechanism

- Topological defects form generically during phase transitions.

- Example: **Domain Walls**

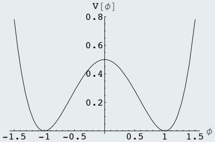

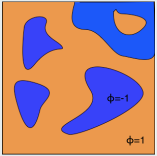

$$\mathcal{L} = \frac{1}{2}\partial_\mu\phi\,\partial^\mu\phi - \lambda(\phi\phi - \eta^2)^2.$$

- The vacuum manifold is given by $\mathcal{M} = \{-1, 1\}$.

The topology of $\mathcal{M}$ determines the type of defects which can form:

$\pi_0(\mathcal{M}) \neq \mathbb{1} \rightarrow$ Domain Walls $\quad \pi_1(\mathcal{M}) \neq \mathbb{1} \rightarrow$ Cosmic Strings

$\pi_2(\mathcal{M}) \neq \mathbb{1} \rightarrow$ Monopoles $\quad \pi_3(\mathcal{M}) \neq \mathbb{1} \rightarrow$ Textures

Textures
The $O(4)-$model

- Textures appear in theories where a non-abelian global symmetry group G is completely broken at low energies.
  - Global $\mathrm{SU}(2)$ symmetry rotating a Higgs doublet.
  - Family symmetry.
- These symmetries are easily implemented in GUT's.
- There are mechanisms where a non-abelian gauge symmetry leads to a global symmetry at low energies. *Turok 90*

The simplest example: $O(4)-$model

$$\mathcal{L} = \frac{1}{2}\partial_\mu\phi_a\,\partial^\mu\phi_a - \lambda(\phi_a\phi_a - \eta^2)^2, \qquad a = 1, \ldots, 4.$$

$$\ddot{\phi}_a - \nabla^2\phi_a = -4\lambda(\phi_b\phi_b - \eta^2)\,\phi_a.$$

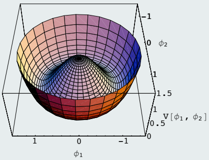

- The model depends on a single parameter:

$$l_\phi \equiv m_\phi^{-1} = (\sqrt{8\lambda}\eta)^{-1}$$

- The vacuum manifold is $\mathcal{M} \cong S^3$.

A texture is a localized region of space where the field ϕ_a winds around $\mathcal{M}$.

- The Higgs lays on the vacuum manifold everywhere in space.

$$\phi_a \phi_a = \eta^2 .$$

- The texture configuration defines a mapping $\mathbb{R}^3 \longrightarrow S^3$.
- Since $\pi_3(\mathcal{M})$ is non-trivial there are configurations which cannot evolve into the homogeneous vacuum.

- There is a conserved topological current:

$$j^\mu = \frac{1}{12\pi^2\eta^4} \epsilon^{\mu\nu\alpha\beta} \epsilon^{abcd} \phi_a \, \partial_\nu \phi_b \, \partial_\alpha \phi_d \, \partial_\beta \phi_d \, , \qquad Q = \int d^3x \, j^0 \in \mathbb{R}.$$

- The charge measures the fraction of $\mathcal{M}$ covered by the texture.

Textures

Spherically symmetric $Q = 1$ configuration

$$\vec{\phi} \equiv (\phi_1, \phi_2, \phi_3) = \eta \sin\chi(r)\,\hat{r}, \qquad \phi_4 = \eta\cos\chi(r).$$

$$\chi(0) = 0, \qquad \chi(r > R) = \pi \quad \Longrightarrow \quad Q = 1.$$

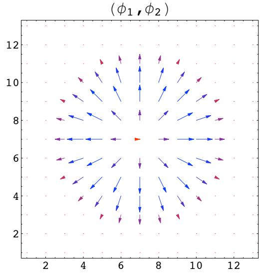

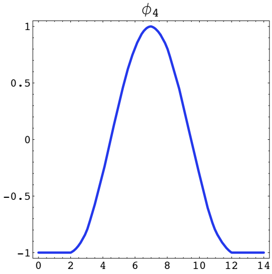

Texture collapse and unwinding
Derrick's theorem

- Consider a localized texture configuration $\phi_a(\vec{r})$.

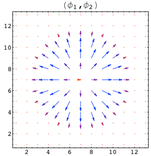

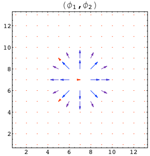

- Transforming the configuration as $\phi_a(\vec{r}) \to \phi_a(\alpha\vec{r})$, with $\alpha > 1$, the energy decreases: **textures are unstable to collapse**.

$$E = \frac{1}{2}\int d^3x\, \vec{\nabla}\phi_a \vec{\nabla}\phi_a \to \alpha^{-1} E$$

- When $R \lesssim l_\phi$ the field gradients pull $\phi_a(\vec{r})$ over the potential barrier.
- The topological charge is no longer conserved and the knot unwinds.
- The energy escapes to infinity in an expanding shell of goldstone bosons.

CMB Anisotropies by Collapsing Textures

Integrated Sachs-Wolfe effect

- Unwinding textures create a time-varying gravitational potential.
- CMB photons crossing it receive a red- or a blue-shift.

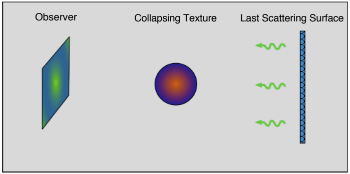

$$\begin{aligned} g_{\mu\nu} &= g^{(0)}_{\mu\nu} + h_{\mu\nu}, \\ \Theta_{\mu\nu} &= \partial_\mu \phi_a \, \partial_\nu \phi_a - g_{\mu\nu} \mathcal{L} \end{aligned}$$

- To first order in the perturbations

$$\frac{\Delta T}{T}(\hat{\mathbf{n}}, \mathbf{x}) = -\tfrac{1}{2} \int_{\lambda_{em}}^{\lambda_{obs}} d\lambda \, h_{ij,0}(\mathbf{x}_\gamma(\lambda)) \; \hat{n}^i \, \hat{n}^j, \quad \mathbf{x}_\gamma(\lambda) = \mathbf{x} - \lambda \hat{\mathbf{n}}$$

  - Matter evolves in the unperturbed background,
  - photons travel along unperturbed trajectories.

CMB Anisotropies by Collapsing Textures

Small-angle approximation

- Metric perturbations can be solved in terms of $\Theta_{\mu\nu}$,
- the anisotropy can be calculated explicitely. *Stebbins et al. 94*

Small-angle approximation

- When the geodesics are almost parallel to the line of sight $\hat{\mathbf{n}}$ *Hindmarsh 94*:

$$\nabla_\perp^2 \frac{\Delta T}{T}(\mathbf{x}_\perp) = -8\pi G \nabla_\perp \cdot \mathbf{U}(\mathbf{x}_\perp)$$

$$U_i(\mathbf{x}_\perp) = -(\delta_i^j - \hat{n}_i \hat{n}^j) \int_{\lambda_{em}}^{\lambda_{obs}} \left[\Theta_{0j}(\mathbf{x}_\gamma(\lambda)) - \hat{n}^k \Theta_{jk}(\mathbf{x}_\gamma(\lambda))\right] d\lambda$$

- Valid for fluctuations on small angular scales.

- These results can be extended to the cosmological case provided
  - the impact parameter of the photons is small compared to H^{-1},
  - the unwinding time is small compared to H^{-1}.

CMB Anisotropies by Collapsing Textures

Cold Spot Formation

Photons crossing the texture *before* the unwinding are *red-shifted*.

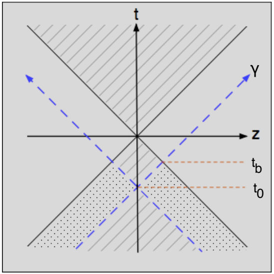

- They fall in the potential well of a fraction of the texture,
- and climb out the potential well of the full texture.

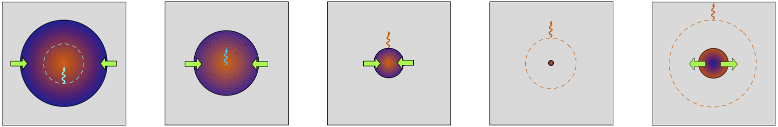

CMB Anisotropies by Collapsing Textures
Hot Spot Formation

Photons crossing the texture *after* the unwinding are *blue-shifted*.

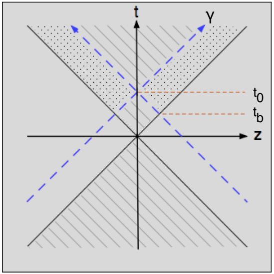

- They fall in the potential well of the full texture,
- and climb out the potential well of a fraction of the texture.

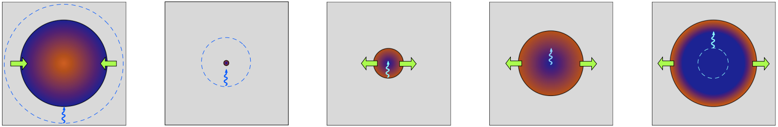

Analytical approach
Non-linear sigma model

- At low energies the massive d.o.f. are not excited, thus $\phi_a(\mathbf{x})$ is constrained to stay in $\mathcal{M}$.

$$\phi_a \phi_a = \eta^2.$$

- We use an effective action with a Lagrange multiplier β:

$$\mathcal{L} = \frac{1}{2}\partial_\mu \phi_a \, \partial^\mu \phi_a - \beta(\phi_a \phi_a - \eta^2).$$

$$\nabla^2 \phi_a + \eta^{-2}(\partial_\mu \phi_b \, \partial^\mu \phi_b)\phi_a = 0.$$

- The effective e.o.m. admit an analytic solution describing a spherically symmetric texture collapse *Turok et al. 90*

$$\vec{\phi} \equiv (\phi_1, \phi_2, \phi_3) = \eta \sin \chi \, \hat{r}, \qquad \phi_4 = \eta \cos \chi.$$

$$\chi(r, t<0) = 2\arctan(-r/t), \quad \chi(r, t>0) = \begin{cases} 2\arctan(r/t) + \pi, & r < t \\ 2\arctan(t/r) + \pi, & r > t. \end{cases}$$

Analytical approach

Non-linear sigma model

Note that:

- Turok's solution extends all the way to spatial infinity,
- and it has a linearly divergent mass:

$$M(r < \Lambda) \sim 8\pi\eta^2\Lambda$$

- The small angle approximation is used implicitly:
  - The photon emission point,
  - the unwinding site,
  - and the observer

  are at an infinite distance from each other.

Analytical approach

Problems of the Self-Similar solution

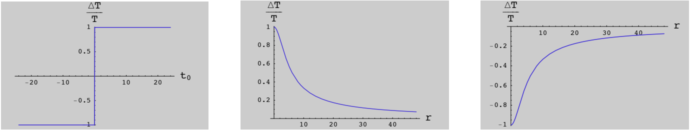

Template used to compare the CMB data with the texture model:

$$\frac{\Delta T}{T}(r, t_0) = \epsilon \, \frac{t_0}{(2r^2 + t_0^2)^{1/2}}, \qquad \epsilon \equiv 8\pi^2 G\eta^2.$$

Turok et al. 90, Stebbins et al. 94

Known problems

- The sigma-model approximation breaks at the unwinding.
- All photons crossing the unwinding site receive the same amount of red/blue-shift, *independently of the time of passing*.
- The anisotropy profile decays very slowly $\sim r^{-1}$.

Analytical approach

Problems of the Self-Similar solution

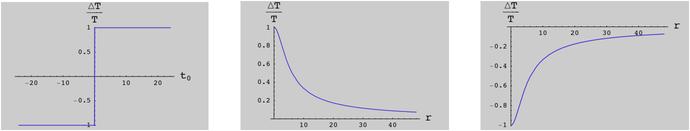

Template used to compare the CMB data with the texture model:

$$\frac{\Delta T}{T}(r, t_0) = \epsilon \, \frac{t_0}{(2r^2 + t_0^2)^{1/2}}, \qquad \epsilon \equiv 8\pi^2 G\eta^2.$$

Turok et al. 90, Stebbins et al. 94

The self-similar solution requires very special initial conditions

- $Q \in \mathbb{Z}$, (in a cosmological context fractional charges are generic.)
- Spherical symmetry.
- A coherent velocity is needed to preserve the self-similar state.

Borrill et al. 92,94

Numerical Methods

Discrete equations of motion

We evolve a discrete version of the $O(4)-$model in a cubic lattice.

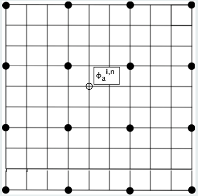

$N = 96^3, \quad \Delta x = 5\Delta t = 4 l_\phi$.

- Fields are evolved in discrete time-steps:

$$\phi_a(\mathbf{x}) \longrightarrow \phi_a^{\mathbf{i},n}.$$

- Derivatives are represented by finite differences:

$$\dot{\phi}_a(\mathbf{x}) \longrightarrow \dot{\phi}_a^{\mathbf{i},n+\frac{1}{2}} = \frac{\phi_a^{\mathbf{i},n+1} - \phi_a^{\mathbf{i},n}}{\Delta t}.$$

- At the edges of the lattice we use periodic boundary conditions,
- we run the simulation for 96 grid units.

- The discrete e.o.m. in a Minkowski background:

$$\dot{\phi}_a^{\mathbf{i},n+\frac{1}{2}} = \dot{\phi}_a^{\mathbf{i},n-\frac{1}{2}} + \left[\nabla^2 \phi_a^{\mathbf{i},n} - 4\lambda(\phi_b^{\mathbf{i},n}\phi_b^{\mathbf{i},n} - \eta^2)\,\phi_a^{\mathbf{i},n} \right] \Delta t$$

$$\phi_a^{\mathbf{i},n+1} = \phi_a^{\mathbf{i},n} + \dot{\phi}_a^{\mathbf{i},n+\frac{1}{2}} \Delta t$$

Numerical Methods

Calculation of the anisotropy

We calculate the anisotropy on a sequence of 48 photon planes

- Planes are separated by one lattice spacing.
- They travel along one of the mayor axis of the lattice.
- Half cross the unwinding site before the event,
- half cross the unwinding site afterwards.

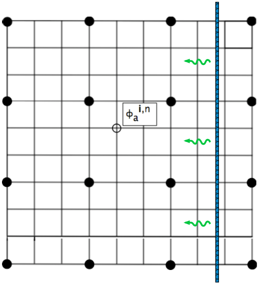

- The anisotropy is calculated from the small-angle formula:

$$\nabla_\perp^2 \frac{\Delta T}{T}(\mathbf{x}_\perp) = -8\pi G \nabla_\perp \cdot \mathbf{U}(\mathbf{x}_\perp),$$

- which is solved using a F.F.T.
- The integration constant is fixed requiring $< \frac{\Delta T}{T} >= 0$. *Borril et al. 94*

Numerical methods

Initial configuration

The initial correlation lenght was set to 16 grid points

- The initial configuration is set assigning random points from $\mathcal{M}$ on a 3^3 sublattice.
- Intermediate points are filled using an algorithm which minimizes the total energy.
- Only a 4% of the initial conditions lead to a texture unwinding.

$$\phi^2 < \eta^2/4, \qquad \textit{Borril et al. 93, 94}$$

- We obtained an ensemble of random initial conditions leading to unwinding events.

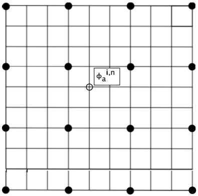

- We evolved 1300 initial conditions,
- obtaining 50 texture unwindings.
- Only 33 were selected for the ensemble,
  - discarding multiple unwinding events and
  - those close to the begining and end of the simulation.

Numerical methods

Limitations of this approach

The evolution of cosmic textures involves physics both at microscopical and cosmological length-scales.

- The microscopical length-scale: $l_\phi = m_\phi^{-1}$
- Cosmological length-scale: $\xi_c \sim H^{-1}$

$$\mathcal{R} = H^{-1}/l_\phi \quad \sim \quad 10^{50}$$

- The asymptotic regime is reached when $\mathcal{R} \sim 200$, *Borril et al. 92*.

Time evolution and radial profile of the anisotropy

Averaged anisotropy profiles:

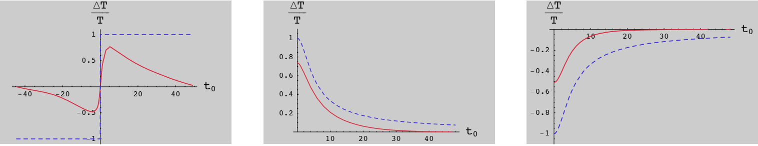

- Textures become spherical close to the collapse. *Turok et al .90*
- Maximum of the hot spot profile $\frac{\Delta T}{T}|_{max} = (+0.77 \pm 0.21)\epsilon$,
- minimum of the cold spot profile $\frac{\Delta T}{T}|_{min} = (-0.49 \pm 0.13)\epsilon$, in agreement with *Borrill et al. 94*
- The unwinding event is resolved, $\delta t \sim 40 l_\phi$.
- The hot and cold spot profile functions are more localized than in the analytic solution.

Time evolution and radial profile of the anisotropy

Averaged anisotropy profiles:

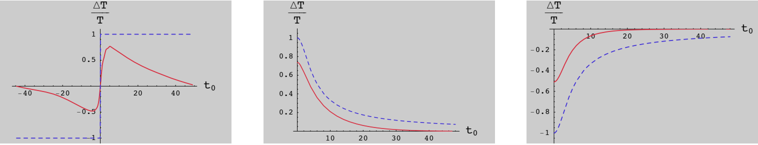

- The brightness of the spot decays at early and late times.
- The CMB analyses depend on the expected number of spots due to textures.

$$N_s(\theta > \theta_c) \quad \Longrightarrow \quad \frac{dN_s}{d\theta_c} \sim \theta^{-3}$$

- This estimate is partially based on numerical simulations which do not consider how photons interact with the texture.
- Our results also indicate a strong dependence on the photon emission and detection times.

Conclusions

Results

- A library of 33 random initial conditions leading to single unwinding events.
- Calculation the corresponding anisotropy profiles using the small-angle approximation.
- The averaged anisotropy pattern is significantly more localized, and has a smaller peak than the Turok solution $(20 - 50\%)$.
- Textures are only observable during a finite interval around the unwinding event.

Conclusions

Results

- A library of 33 random initial conditions leading to single unwinding events.
- Calculation the corresponding anisotropy profiles using the small-angle approximation.
- The averaged anisotropy pattern is significantly more localized, and has a smaller peak than the Turok solution $(20 - 50\%)$.
- Textures are only observable during a finite interval around the unwinding event.

To be done:

- Repeat the simulations in a FRW background.
- Resimulate in a larger lattice to increase precision and diminish boundary effects.
- Characterize the small scale anisotropies due to random fluctuations of the fields.